Original Article: Novel Modified Magnetic Mesopouros Silica for Rapid and Efficient Removal of Methylene Blue Dye from Aqueous Media

Kamal Alizadeh [a,*] | Esmail Khaledyan [b] | Yagoub Mansourpanah [a]

[a]*Department of Chemistry, Lorestan University, Khorramabad 6813717133, Iran*

[b] *Department of Chemistry, Lorestan University, Khorramabad, Iran*

Use your device to scan and read the article online

Citation K. Alizadeh*, E. Khaledyan, Y. Mansourpanah. **Novel Modified Magnetic Mesopouros Silica for Rapid and Efficient Removal of Methylene Blue Dye from Aqueous Media**. *J. Appl. Organomet. Chem.*, **2022**, *2*(4), 198-208.

https://doi.org/10.22034/jaoc.2022.155004

Article info:
Received: 2022-05-12
Accepted: 2022-06-11
Available Online: 2022-07-29

Checked for Plagiarism: Yes

Editor who Approved Publication:
Professor Dr. Abdelkader Zarrouk

Keywords:
Methylene blue; Magnetic mesoporous silica sorbent; Adsorption; Removal; Fe_3O_4@MCM-41@ MAA-APTES

ABSTRACT

This reaserch aims at functionalizing magnetic mesoporous silica with methacrylic acid-3-aminopropyltriethoxysilane (Fe3O4@MCM-41@MAA-APTES) applied for removal of methylene blue from aqueous solution. Several variables (such as pH, dye concentration, adsorbent amount and contact time) have been investigated. Under optimum conditions, maximum capacity of 87.71 mg g-1 of MB was obtained for the sorbent. The magnetic mesoporous silica was characterized by SEM, FT-IR, XRD and VSM analyses. The adsorption isotherms were also studied for the sorbent and Langmuir model was found to be more applicable in interpreting MB adsorption on the magnetic nanocomposite silica. The pseudo-second order kinetic model adequately described the kinetic data.

Introduction

Recently, the issue of environmental pollution has becomes a global concern [1]. Discharging wastewater that contains organic dyes from some industries such as textiles, paper, rubber, plastics, cosmetics, etc, is one of the major sources of pollutants to water reservoirs. Presence of organic dyes, even in trace levels, can be harmful for public health and damage the environment [2-4]. Most synthetic dyes have a complex aromatic molecular structure which makes them more stable and difficult to decompose [5] and also potential toxicity, carcinogenicity and mutagenicity [6]. Methylene blue(MB) is a cationic dye (Formula weight 319.86 g mol^{-1}, λ_{max}= 665 nm) that has been widely used in dying cotton, wood, and silk. Different physical, chemical and biological methods can be used to remove dyes from wastewater [7]. Some of them involve

*Corresponding Author: : Kamal Alizadeh (Alizadehkam@yahoo.com, Alizadeh.k@lu.ac.ir)

coagulation, foam flotation, ion exchange, sedimentation, solvent extraction, adsorption, electrolysi,chemical oxidation, disinfection, chemical precipitation, and membrane process [8,9]. The adsorption .
technique is an interesting method because it has been found to be more effective and low-cost treatment process to remove the synthetic dyes [10,11].The most important adsorbents applied in wastewater treatment are activated carbon [12], nanocomposites [13,14], chitosan [15] and iron oxide nanomaterial [16]. Iron oxide nanomagnet has attracted much consideration for removing the dye pollutants due to its efficient treatment of large-volume water of samples, and easily separable by usingan external magnetic field [17-19]. Due to its unique characteristics such as large surface area, high porosity, controllability and uniform pore size modified mesoporous silica has been attracted in many field of researchs in recent years [20-22]. Organic functionalizing of the pore wall of in mesoporous silica containing amine and thiol groups led to rapid and high capacity of absorption as well as the selectivity [23]. The most common types of mesoporous nanoparticles are MCM-41, MCM-48 and SBA-15. The magnetic nanoparticles can be encapsulated into the mesoporous silica with suitable properties such as stability, collected by the use of external magnetic and ease of further surface modification. Magnetic mesoporous silica nanoparticles consist of magnetic nanoparticle core and a mesoporous silica shell. The aim of this study is the investigation of removal of MB using synthesis magnetic nanocomposite by means of modifying its surface.

.

Experimental materials and methods

Chemical and materials

The chemicals, cetyltrimethylammonium bromide(CTAB) (99%), HCl (37%), acetic acid glacial(99%), NaOH, methylene blue(MB), and ammonia solution (25%) were purchased from Merck, Germany. Tetraethylorthosilicate (TEOS, ≥98%), methacrylic acid (MAA, ≥99%) and 3-aminopropyltriethoxysilane (APTES, ≥98%) were purchased from Sigma-Aldrich (USA). The chemical structure of MB is shown in Figure 1

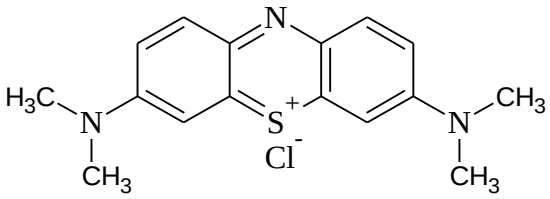

Figure 1. Chemical structure of MB

Instruments

UV-Visible absorption was performed using a double beam UV-Visible spectrophotometer (Shimadzu model 1800, Japan). The morphological structure of nanocomposite was characterized by a Scanning Electron Microscope (SEM) model FE-SEM from Tescan Company. Fourier FT-IR spectrum was recorded on a Shimadzu, Fourier transform infrared spectroscopy (FT-IR) spectrometer model 8400S (Japan). The magnetic measurements were carried out in a vibrating sample magnetometer (VSM, MDKB, Daghigh Meghnati Kavir Co., Iran) at room temperature. XRD patterns were obtained by X-ray diffractometer (Perkin Elmer-USA).

Preparation of MAA-APTES monomers

The MAA-APTES monomers (for surface modification of magnetic nanocomposite) were synthesized according to the previously reported method [24]. Briefly, the MAA-APTES monomers were synthesized by addition 6.4 mmol of APTES and 8.1 mmol of MAA and were heated at 60 ^{0}C for 24 h.

Preparation of magnetic mesoporous

In second step, the Fe_3O_4 nanoparticle was prepared by co-precipitation method [25]. In

this method, mixture of chloride salts of $F[e^{+2}$ and Fe^{+3} ions with molar ratio 1:2
was added in an ammonium hydroxide solution into 100 mL three neck flask under N_2 atmosphere and stirring condition. The product was collected by magnet and washed three times by double distilled water and dried at 70 ^{0}C using vacuum oven.
In the next step, the dried Fe_3O_4 nanoparticle was used to prepare magnetic nanomesoporos with Stöber method [26]. 0.5 gr of magnetic nanoparticle was dispersed in mixture of ethanol and deionized water with ratio of 1:2. The resulting mixture was homogenized for 30 min by placing in an ultrasonic bath at constant temperature (25 ^{0}C). To this mixture, 1.2 mL of ammonia solution (25%) was added and stirred for 1 h. Then, a 100 mmol/l of CTAB solution was added dropwise and stirred in room temperature for 1 h. After that, 1.05 gr of TEOS was added to the mixture and stirred for 24 h. The resulting product was collected by magnet and repeatedly washed with mixture of deionized water/ethanol to remove any residue. Finally, the magnetic nanocomposite product was dried in room temperature for 24 h. The obtained magnetic nanocomposite was calcinate at 550 ^{0}C for 6 h in the air atmosphere.

For the surface modification of magnetic nonporous with MAA-APTES monomers, 2 mL of MAA-APTES monomers was added to 20 mL of ethanol, and 0.2 gr of magnetic nanocomposite was added to the mixture and the reaction mixture was allowed to react by refluxing at 70 ^{0}C for 4 h under continuous stirring at 150 rpm. Thereafter, the modified magnetic mesoporous silica were collected by using magnet and washed sequentially with ethanol and deionized water. The Fe_3O_4@MCM-41@ MAA-APTES was dried at room temperature for 24 h.

Dye removal procedure

In each experimental removal, 0.01gr of adsorbent was added to 25 mL of 20 mg/L dye. The pH of solutions adjusted 7 with 0.010 M HCl and 0.01M NaOH solutions. The mixture was shaken at 150 rpm for 3.5 min at room temperature. The adsorbent was separated by applied external magnetic. The remained MB in solution was determined at maximum absorption by a UV-Vis spectrophotometer. The amount of dye adsorbed onto the adsorbent at equilibrium (Q_e) and percentage of dye removal was calculated using the following equations:

$$Q_e = \frac{(C_0 - C_t)V}{m} \quad (1)$$

$$\text{Dye removal (\%)} = \frac{(C_0 - C_e)100}{C_0}$$

in which C_0 and C_e (mg/L) are the initial and equilibrium concentrations of MB in the solution, V(L) is volume of dye solution and m (gr) is the mass of the adsorbent.

Desorption and reusability

To evaluate the reusability of the modified magnetic mesoporous silica nanoparticles (MMMSN), 0.01 g of the MMMSN was added to 25 mL of the 20 mg/L of the MB solution and the mixture was stirred at 150 rpm for 3.5 min. The MMMSN was collected from solution using external magnet and added in the 5 mL of 0.1M acetic acid and stirred for about 5 min. After desorption MB, the MMMSN was collected and amount of desorbed MB was determine using a UV-Vis spectrophotometer. The result showed that the recovery values were not decreased after several times of successive extraction process that demonstrates the stability of sorbent. Scheme 1 shows the operation steps.

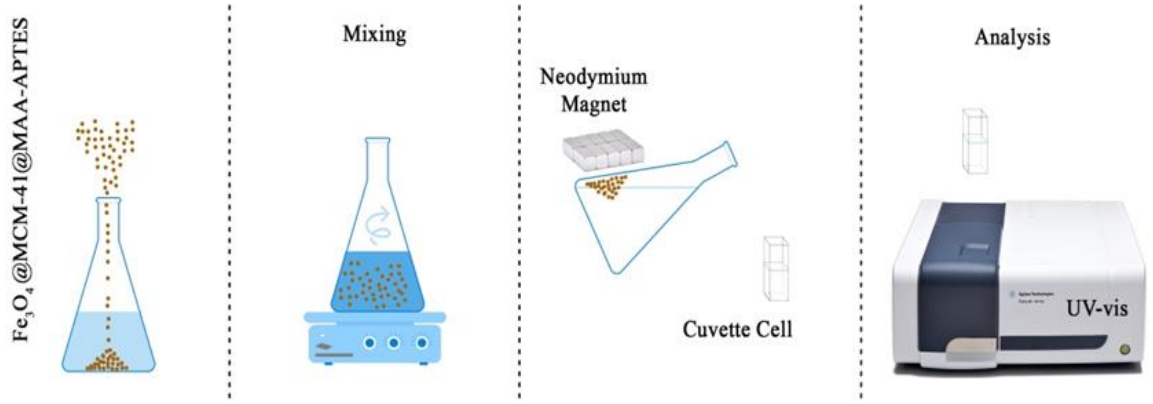

Scheme 1. Experiment steps of the rapid removal of methylene blue from various natural samples using magnetic mesoporous silica *Fe_3O_4@MCM-41@MAA-APTES* modified by methacrylic acid-3-aminopropyltriethoxysilane(MAA-APTES) is shown from left to right respectively.

Results and Discussion

Characterization of Fe_3O_4@MCM-41@ MAA-APTES

The Fe_3O_4 nanoparticle, Fe_3O_4@MCM-41-NH_2 and Fe_3O_4@MCM-41@MAA-APTES were characterized by XRD technique. The XRD patterns of the Fe_3O_4 show eight diffraction peaks corresponding to typical reflection of (220), (311), (400), (422), (511), (440), and (533) crystallographic planes of Fe_3O_4. When Fe_3O_4 coated by silica and modified with monomer (MAA-APTES), it had similar diffraction peaks (Figure 2) corresponding cubic spinel crystal structure that show no change in the crystal structure and indicating preservation of the magnetic core.

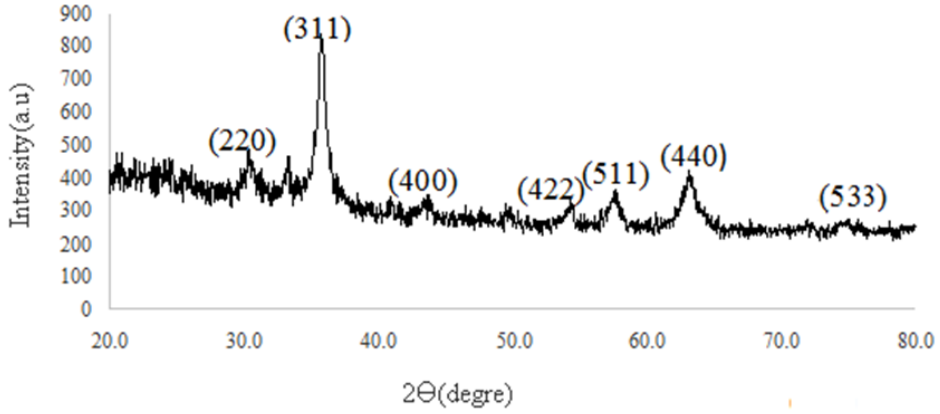

Figure 2. XRD pattern of Fe_3O_4@MCM-41@MAA-APTES

The coated MAA-APTES on the magnetic nanocomposite silica could be detected by FT-IR techniques. Figure 3 shows the FTIR spectra of Fe_3O_4@MCM-41, Fe_3O_4@MCM-41-NH_2 and Fe_3O_4@MCM-41@MAA-APTES. The FT-IR spectrum of Fe_3O_4@MCM-41 (Figure 3a) appeared in 790, 960 and 1080 cm^{-1} that correspond to stretching vibration symmetric and asymmetric stretching of Si-O-Si band, respectively. The FT-IR spectrum of Fe_3O_4@MCM-41-NH_2 has been shown in Figure 3b. Two broad absorption peaks at 2931 and 1618 cm^{-1} were belonged to $-CH_2$ stretching and bending vibration of N-H. Figure 2c shows the FT-IR spectra of the modified magnetic mesoporous silica with monomer MAA-APTES. Two absorption peaks at 1637 and 3386 belonged to amide stretching vibration and N-H, respectively. The results of FT-IR indicated that the synthesized monomer has been successfully coated on the surface of magnetic mesoporous

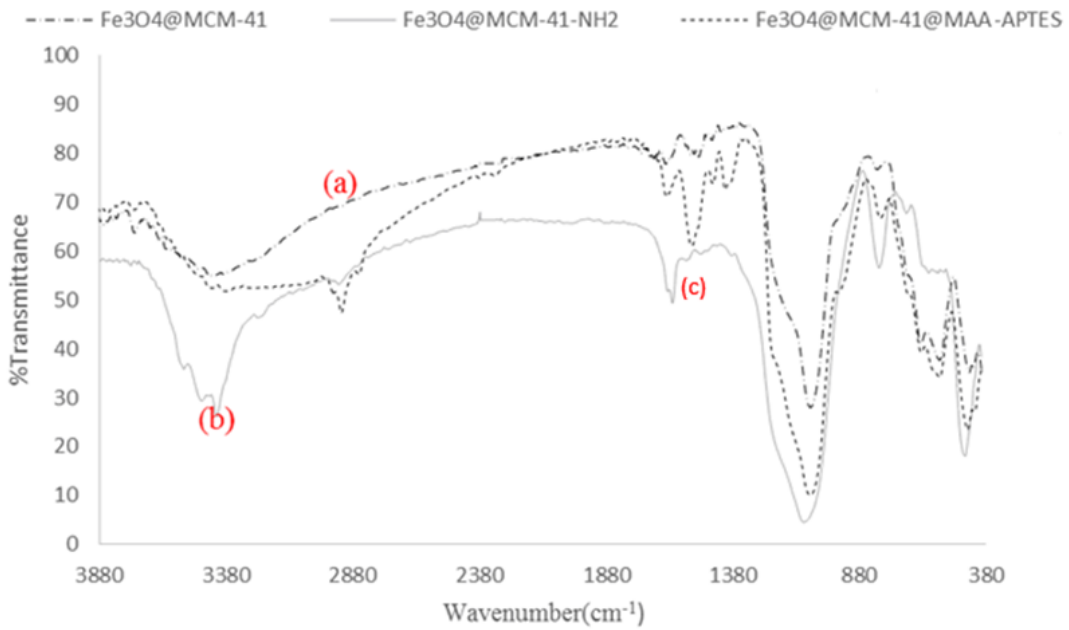

Figure 3. FT-IR spectra of synthesis magnetic mesoporous silica

The shape, morphology and size of the magnetic composite silica were obtained by SEM measurements. The FESEM image (Figure 4) shows that magnetic composite silica has nearly spherical shape and a relatively smooth uniform surface.

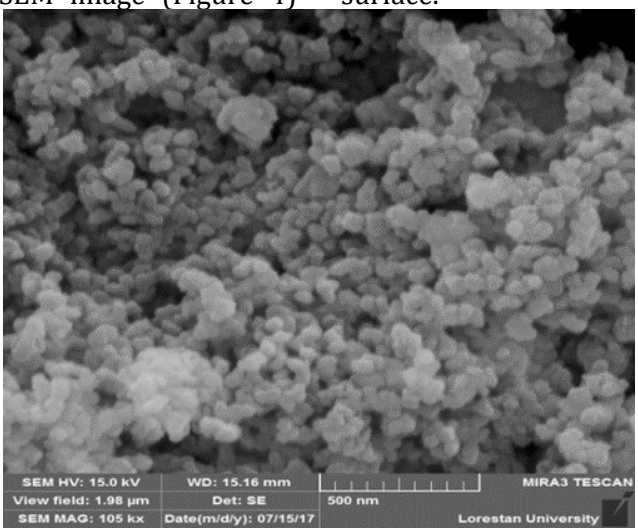

Figure 4. SEM image of Fe_3O_4@MCM-41@MAA-APTES

The magnetization curve of the Fe_3O_4@MCM-41 and Fe_3O_4@MCM-41@MAA-APTES nanoparticles recorded with VSM are shown in Figure 5. The magnetization of nanoparticles would approach the saturation values when the applied magnetic field increases to more than 8000 Oe. The saturation magnetization of the Fe_3O_4@MCM-41 and Fe_3O_4@MCM-41@MAA-APTES was 27.73 and 18.32 emu/g respectively. These results show that the magnetic properties are affected by surface modification of Fe_3O_4@MCM-41 with MAA-APTES.

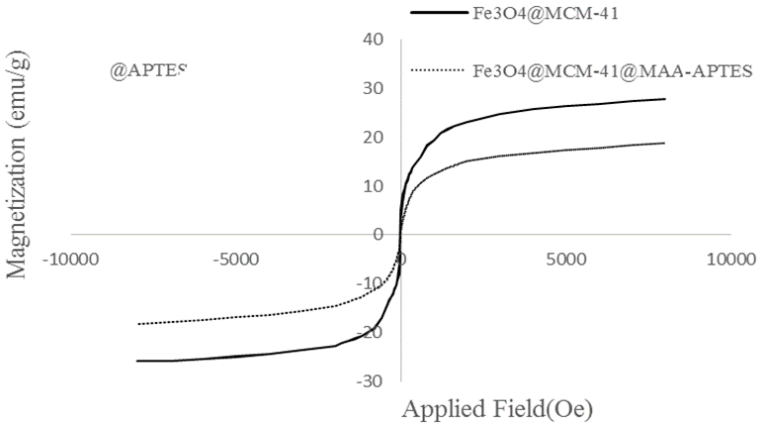

Figure 5. Magnetic curves of the Fe3O4@MCM-41 (____) and Fe3O4@MCM-41@MAA-APTES (____)

Effect of pH

The quantity of pH has main role on dyes removal from aqueous solution. The effect of the pH on the adsorption of MB was investigated in the range of 4-11. As indicated in Figure 6, removal of MB gradually increase as function of pH. In acidic pH, there is a competition between hydronium and MB for binding adsorption sites. As pH increases, various interactions among polar functional groups and π-π interactions will happen on the surface of MMMSN which result in increasing adsorption cationic MB. Thus, similar to some previous reports [27,28], we suppose that the binding mechanism of cationic methylene blue dye on the surface of the nanocomposite is most likely to be due to electrostatic interactions between the positively charged sulfur group of dye(MB) with the negatively charged surface of the nanocomposite(Fe3O4@MCM-41@MAA-APTES) in the optimized pH (≈9).

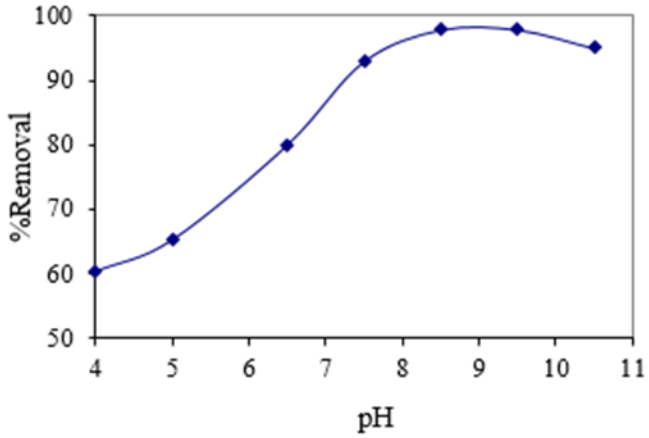

Figure 6. Effect of pH on the removal of MB at room temperature Fe_3O_4@MCM-41@MAA-APTES

Effect of MMMSN dosage

Figure 7 shows the effect of the MMMSN dosage on MB removal from the solution. In the present work, for optimizing the amount of MMMSN, the concentration of MB, pH and stirring time were fixed at 32 mg/L, 9 and 3.5 min, respectively, in the room temperature and the dosage of adsorbent varied from 2-35 mg. The result shows that the percentage removal of MB increase from 35 to 97 % with increasing dosage of adsorbent. This results indicate that increasing in the amount of MMMSN led to increases the removal efficiencies of MB due to the availability of higher adsorption sites.

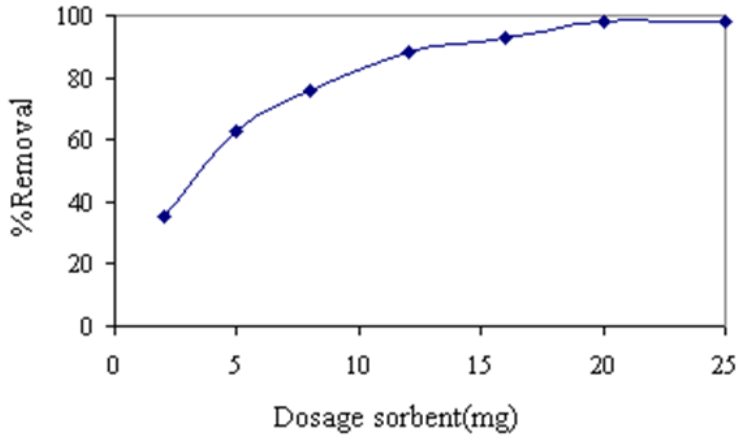

Figure 7. Effect of amount of adsorbent (g) on MB removal at room temperature by Fe_3O_4@MCM-41@MAA-APTES

Effect of contact time

As shown in Figure 8, the uptake efficiency of MB by adsorbent initially increased with time due to the availability of numerous active adsorption sites. The rate of removal was decreased due to the decreasing number of availability of active sites.

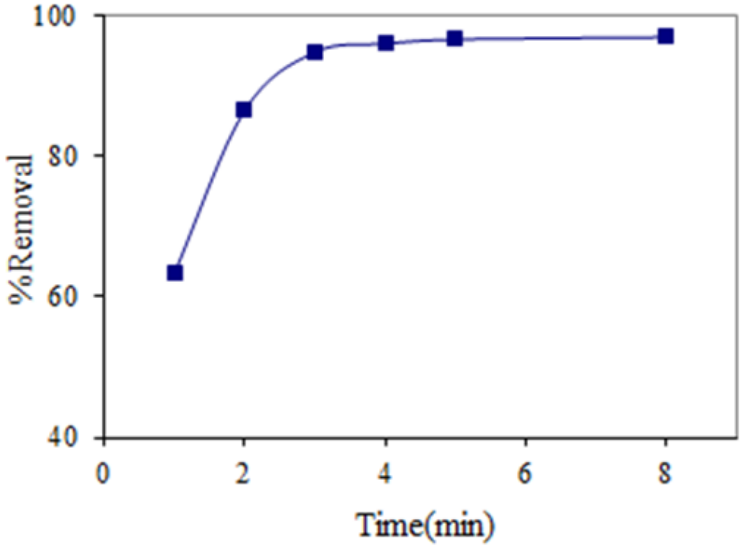

Figure 8. Effect of contact time of removal MB on Fe_3O_4@MCM-41@MAA-APTES

Effect of initial MB concentration

The uptake efficiency of MB by MMMSN depends on the initial MB concentration from 4 to 50 mg/L, as the dosage of adsorbent was 0.01 gr in 25 mL. The results shown in Figure 9 indicate that with increasing in the concentration of MB in solution, the removal efficiency was decreased.

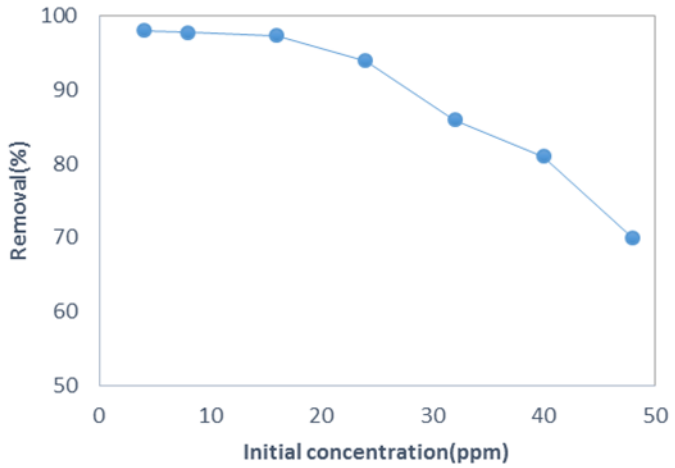

Figure 9. The effect of initial MB concentration on percent removal

Adsorption isotherms

The equilibrium isotherm models are known as effective method to understand the adsorption mechanism and how adsorbate and adsorbent interact with each other. In this work, two common models, Longmuir [29] and Freundlich [30] were investigated. This models can be expressed by Eqs. (3) and (4), respectively:

$Qe=q_m bC_e/(1+bC_e)$ (3)

$Ln\ (q_e) = LnK_F + LnC_e$ (4)

Where Q_e (mg/L) is the amount of MB uptake by MMMSN in equilibrium, C_e (mg/L) is the equilibrium concentration of MB, q_m (mg g^{-1}) the monolayer capacity of the adsorbent, K_L and K_F are constant equilibrium of models Longmuir and Freundlich, respectively.

Table 1. Langmuir and Freundlich isotherm constants and related correlation coefficients

Langmuir model			**Freundlich model**		
q_{max} (mg.g^{-1})	K_L (L.mg^{-1})	R^2	K_F (mg.g^{-1})	n	R^2
87.71	0.048	0.9118	4.49	1.59	0.6927

Adsorption kinetics

To understand the adsorption process, it is necessary to study the removal process. Absorption of absorbent material on the adsorbent may include several steps including film release, intrinsic emission, surface diffusion and pore-level adsorption, or a combination of several steps. In this study, four model kinetics such as first pseudo order [31], second pseudo order [31], diffusion particle [32] and Elovich [33] model have been investigated. In order to carry out kinetics studies, the amount of dye absorption per unit mass of absorbent during equilibrium is calculated from the following equation:

$Q_e= (C_e-C_0)\ V/M$ (5)

Where C_e is the amount of dye at equilibrium and C_0 is the initial concentration, V is volume and M is the amount of adsorbent. The linear equations of this models are respectively shown in Eqs. (6-9):

$$\log(q_e - q_t) = \log q_e - \frac{K_1}{2.303} t \quad (6)$$

$$\frac{t}{q_t} = \frac{1}{K_2 q_e^{\ 2}} + \frac{t}{q_e} \quad (7)$$

$$q_t = K_{diff} t^{1/2} + C \quad (8)$$

$$q_t = \frac{1}{\beta}\ln(\alpha\beta) + \frac{1}{\beta}\ln t \quad (9)$$

Where q_e and q_t are the amount of MB adsorbed in equilibrium and contact time t (min), respectively. K_1 is the rate constants of first pseudo order and K_2 is the rate pseudo second order model. K_{diff} is the rate constant in the intra-particle diffusion model. The kinetics parameters were calculated and given in Table 2.

The obtained results showed that the experimental data had better fit to the pseudo-second order kinetics model base on the correlation coefficient values that presented in Table 2.

Table 2. Kinetic parameters for removal of MB solution

Model	parameters	Concentration of MB
		15
pseudo-first order kinetic	$k_1(min^{-1})$	**0.327**
	$q_e(calc(mg.g^{-1}))$	**22.85**
	R^2	**0.9826**
pseudo-second-order kinetic	$k_2(min^{-1})$	**0.046**
	$q_e(calc(mg.g^{-1}))$	**52.083**
	R^2	**0.9969**
Intrapartcle diffusion	$K_{diff}(mg.g^{-1}.min^{-1/2})$	**14.45**
	R^2	**0.9505**
Elovich	α	**2.0491**
	β	**0.084**
	R^2	**0.9804**

Comparison

Table 3 gives a comparison of this study with some previously reported results in term of adsorption capacity and contact time and amount of adsorbent. The amount of adsorbent and contact time for this method in comparison with other reported methods is preferable.

Table 3. Comparison of various adsorbents for removal MB from water solutions

Adsorbent	Amount of adsorbent	$q_{max(mg/g)}$	time(min)	**Ref.**
ZnS:Cu-NP-AC	0.04	106.9	2.2	[34]
Ag NPs-AC	0.022	71.43	15	[35]
Pd-NPs-AC	0.022	75.40	15	[35]
CuO-NP-AC	0.090-0.11	10.55	15	[36]
ATP@CCS	0.075	226.24	480	[37]
QDs-MSN	0.62	73.15	5	[38]
Fe_3O_4@MCM-41@MAA-APTES	0.005-0.025	87.71	3.5	Our work

Conclusion

In this work, for the first time, magnetic mesoporous nanoparticle was functionalized by MAA-APTES monomers and it was utilized as novel adsorbent for the efficient, selective and rapid removal of MB. The effects of various parameters such as solution pH, initial concentration of MB, dosage of adsorbent and contact time was investigated. At optimum condition, the maximum efficiency removal of MB 97 % was obtained. The value of maximum adsorption capcity, q_{max} was found 87.71 for about 3.5 min. The adsorbent was prepared and characterized for its surface properties. The equilibrium data were best described by the Langmuir model, while the appropriate kinetic model for fitting the experimental data is pseudo-second order model.

Acknowledgements

The authors gratefully acknowledge the Lorestan University for supporting and encouragements.

References

[1] J. Paul, K. Rawat, K. Sarma, S. Sabharwal, *Appl. Radiat. Isot.,* **2011**, *69*, 982-987. [Crossref], [Google Scholar], [Publisher]
[2] T. Pekdemir, B. Keskinler, E. Yildiz, G. Akay, *J. Chem. Technol. Biot.,* **2003**, *78*, 773-780. [Crossref], [Google Scholar], [Publisher]
[3] E.J. Weber, V.C. Stickney, *Water Res.*, **1993**, *27*, 63-67. [Crossref], [Google Scholar], [Publisher]
[4] M.R. Mello, D. Phanon, G.Q. Silveira, P.L. Llewellyn, C.M. Ronconi, *Micropor. Mesopor. Mat.*, **2011**, *143*, 174-179. [Crossref], [Google Scholar], [Publisher]
[5] T. Robinson, G. McMullan, R. Marchant, P. Nigam, *Bioresour. Technol.,* **2001**, *77*, 247-255. [Crossref], [Google Scholar], [Publisher]
[6] Z. Aksu, *Process Biochem.*, **2005**, *40*, 997-1026. [Crossref], [Google Scholar], [Publisher]
[7] M. El Haddad, R. Slimani, R. Mamouni, S. ElAntri, S. Lazar, *J. Assoc. Arab Univ. Basic Appl. Sci.,* **2013**, *14*, 51-59. [Crossref], [Google Scholar], [Publisher]
[8] H. Wang, X. Yuan, G. Zeng, L. Leng, X. Peng, K. Liao, L. Peng, Z. Xiao, *Environ. Sci. Pollut. Res. Int.,* **2014**, *21*, 11552-11564. [Crossref], [Google Scholar], [Publisher]
[9] C.K. Araújo, G.R. Oliveira, N.S. Fernandes, C.L. Zanta, S.S.L. Castro, D.R. da Silva, C.A. *Environ. Sci. Pollut. Res.*, **2014**, *21*, 9777-9784. [Crossref], [Google Scholar], [Publisher]
[10] E. Forgacs, T. Cserhati, G. Oros, *Environ. Int.,* **2004**, *30*, 953-971. [Crossref], [Google Scholar], [Publisher]
[11] E.C. Lima, B. Royer, J.C. Vaghetti, N.M. Simon, B.M. da Cunha, F.A. Pavan, E.V. Benvenutti, R. Cataluña-Veses, C. Airoldi, *J. Hazard. Mater.,* **2008**, *155*, 536-550. [Crossref], [Google Scholar], [Publisher]
[12] P.K. Malik, *J. Hazard. Mater.,* **2004**, *113*, 81-88. [Crossref], [Google Scholar], [Publisher]
[13] M. Hua, S. Zhang, B. Pan, W. Zhang, L. Lv, Q. Zhang, *J. Hazard. Mater.,* **2012**, *211*, 317-331. [Crossref], [Google Scholar], [Publisher]
[14] F. Han, V.S.R. Kambala, M. Srinivasan, D. Rajarathnam, R. Naidu, *Appl. Catal. A-Gen.,* **2009**, *359*, 25-40. [Crossref], [Google Scholar], [Publisher]
[15] V. Gupta, P. Carrott, M. Ribeiro Carrott, Suhas, *Crit. Rev. Env. Sci. Tec.,* **2009**, *39*, 783-842. [Crossref], [Google Scholar], [Publisher]
[16] P. Xu, G.M. Zeng, D.L. Huang, C.L. Feng, S. Hu, M.H. Zhao, C. Lai, Z. Wei, C. Huang, G.X. Xie, *Sci. Total Environ.,* **2012**, *424*, 1-10. [Crossref], [Google Scholar], [Publisher]
[17] S. Zhang, H. Niu, Z. Hu, Y. Cai, Y. Shi, *J. Chromatogr. A,* **2010**, *1217*, 4757-4764. [Crossref], [Google Scholar], [Publisher]
[18] X. Zhao, J. Wang, F. Wu, T. Wang, Y. Cai, Y. Shi, G. Jiang, *J. Hazard. Mater.,* **2010**, *173*, 102-109. [Crossref], [Google Scholar], [Publisher]
[19] L.H. Luo, Q.M. Feng, W.Q. Wang, B.L. Zhang, Fe3O4/Rectorite composite: preparation, characterization and absorption properties from contaminant contained in aqueous solution, in: Advanced Materials Research, Trans Tech Publ,

2011, pp. 592-598. [Crossref], [Google Scholar], [Publisher]
[20] A. Çıtak, B. Erdem, S. Erdem, R.M. Öksüzoğlu, *J. Colloid Interf. Sci.,* **2012**, *369*, 160-163. [Crossref], [Google Scholar], [Publisher]
[21] S. Rostami, S.N. Azizi, N. Asemi, *Iran. Chem. Commun.,* **2019**, *7*, 20-42. [Crossref], [Google Scholar], [Publisher]
[22] B. Khodavirdilo, N. Samadi, R. Ansari, *Iran. Chem. Commun.,* **2019**, *7*, 71-78. [Crossref], [Google Scholar], [Publisher]
[23] T. Yokoi, Y. Kubota, T. Tatsumi, *Appl. Catal. A-Gen.,* **2012**, *421*, 14-37. [Crossref], [Google Scholar], [Publisher]
[24] H. Yan, M. Wang, Y. Han, F. Qiao, K.H. Row, *J. Chromatogr. A,* **2014**, *1346*, 16-24. [Crossref], [Google Scholar], [Publisher]
[25] E. Tahmasebi, Y. Yamini, S. Seidi, M. Rezazadeh, *J. Chromatogr. A,* **2013**, *1314*, 15-23. [Crossref], [Google Scholar], [Publisher]
[26] W. Stöber, A. Fink, E. Bohn, *J. Colloid Interf. Sci.,* **1968**, *26*, 62-69. [Crossref], [Google Scholar], [Publisher]
[27] E. Khaledyan, K. Alizadeh, Y. Mansourpanah, *Iran. J. Sci. Technol. Trans. A: Sci.,* **2019**, *43*, 801-811. [Crossref], [Google Scholar], [Publisher]
[28] K. Alizadeh, E. Khaledyan, Y. Mansourpanah, *J. Water Environ. Nanotechnol.,* **2018**, *3*, 243-253. [Crossref], [Google Scholar], [Publisher]
[29] W.J. Weber, J.C. Morris, *J. Sanit. Eng. Div.,* **1963**, *89*, 31-60. [Crossref], [Google Scholar], [Publisher]
[30] I. Langmuir, *J. Am. Chem. Soc.,* **1916**, *38*, 2221-2295. [Crossref], [Google Scholar], [Publisher]
[31] M. Mansour, M. Ossman, H. Farag, *Desalination,* **2011**, *272*, 301-305. [Crossref], [Google Scholar], [Publisher]
[32] Y.-S. Ho, G. McKay, *Process Saf. Environ. Prot.,* **1998**, *76*, 183-191. [Crossref], [Google Scholar], [Publisher]
[33] M. Ghaedi, A. Ghaedi, E. Negintaji, A. Ansari, A. Vafaei, M. Rajabi, *J. Ind. Eng. Chem.,* **2014**, *20*, 1793-1803. [Crossref], [Google Scholar], [Publisher]
[34] A. Asfaram, M. Ghaedi, S. Hajati, M. Rezaeinejad, A. Goudarzi, M.K. Purkait, *J. Taiwan Inst. Chem. Eng.,* **2015**, *53*, 80-91. [Crossref], [Google Scholar], [Publisher]
[35] M. Roosta, M. Ghaedi, A. Daneshfar, R. Sahraei, A. Asghari, *Ultrason. Sonochem.,* **2014**, *21*, 242-252. [Crossref], [Google Scholar], [Publisher]
[36] M. Ghaedi, A. Ghaedi, M. Hossainpour, A. Ansari, M. Habibi, A. Asghari, *J. Ind. Eng. Chem.,* **2014**, *20*, 1641-1649. [Crossref], [Google Scholar], [Publisher]
[37] Q. Zhou, Q. Gao, W. Luo, C. Yan, Z. Ji, P. Duan, *Colloids Surf. Physicochemical Eng. Aspects,* **2015**, *470*, 248-257. [Crossref], [Google Scholar], [Publisher]
[38] D. Dutta, D. Thakur, D. Bahadur, *Chem. Eng. J.,* **2015**, 281, 482-490.[Crossref], [Google Scholar], [Publisher]